Biodesign

pISSN 2288-6982 | eISSN 2288-7105

CRYSTALLIZATION P 78-81

Purification, crystallization and X-ray crystallographic analysis of *meso*-diaminopimelic acid decarboxylase from *Corynebacterium glutamicum*

Hyeoncheol Francis Son and Kyung-Jin Kim*

School of Life Sciences, KNU Creative BioResearch Group, Kyungpook National University, Daehak-ro 80, Buk-ku, Daegu 41566, Korea. *Correspondence: kkim@knu.ac.kr

meso-Diaminopimelic acid decarboxylase from *Corynebacterium glutamicum* (*Cg*DAPDC) is the key enzyme for the production of L-lysine and it catalyzes *meso*-DAP to produce the final product, L-lysine. The *Cg*DAPDC was overexpressed and purified to homogeneity by Ni-NTA affinity and size-exclusion chromatography. The *Cg*DAPDC protein was crystallized using sitting-drop vapor-diffusion method in the presence of 0.8 M sodium citrate tribasic and 0.1 M sodium cacodylate, pH 6.5 at 293 K. X-ray diffraction data were collected to a maximum resolution of 2.4 Å. The crystal belonged to space group $P2_12_12$, with unit cell parameters a = 114.54 Å, b = 91.702 Å, c = 95.161, $\alpha = \beta = \gamma = 90°$. With one molecules per asymmetric unit, the crystal volume per unit protein mass was 2.64 $Å^3$ Da^{-1}, which correspond to a solvent content of approximately 53.37%.

INTRODUCTION

Corynebacterium glutamicum was first described in 1896, and the whole genome sequence analysis of *C. glutamicum* ATCC 13032 was completed in 2003 (Ikeda and Nakagawa, 2003; Kalinowski et al., 2003; Lehmann, 1896). *C. glutamicum* is generally recognized as a safe (GRAS) organism used in industrial biotechnology, and especially, *C. glutamicum* has been widely used to produce amino acids such as L-glutamate and L-lysine, and other chemicals such as cadaverine, ethylene glycol, and isobutanol (Becker and Wittmann, 2012; Blombach et al., 2011; Buschke et al., 2011; Chen et al., 2016; Huang et al., 2017; Wendisch et al., 2016).

L-lysine is an essential amino acid that has been used as a feed additive with L-methionine, L-threonine, and L-tryptophan, and can be converted into other high value bio-molecules such as diaminopentane and poly-ε-lysine (Mimitsuka et al., 2007; Sagong and Kim, 2017; Sagong et al., 2016). The de novo L-lysine biosynthetic pathway, starting form aspartate, is followed by a four-step enzyme reaction to produce tetrahydropicolinate (THDP). THDP is then converted to *meso*-diaminopimelic acid (*meso*-DAP) through four different pathways such as succinyl-, acetyl-, dehydrogenases-, and aminotransferase pathway, and in *C. glutamicum*, succinyl- and dehydrogenase pathways are used to produce *meso*-DAP. As a final step in the L-lysine biosynthesis, *meso*-DAP decarboxylase (DAPDC) catalyzes *meso*-DAP to produce the final product, L-lysine (Figure 1).

The DAPDC enzyme reacts with pyridoxal 5'-phosphate (PLP) as a cofactor. PLP is one of the active forms of vitamin B6, and enzymes using PLP as cofactor can be classified into five types based on protein structures (Kumar, 2016; Percudani and Peracchi, 2003). Each type of PLP dependent enzymes has aminotransferase and decarboxylase (DC) (type I), β-elimination (type II), alanine racemase (type III), D-amino acid

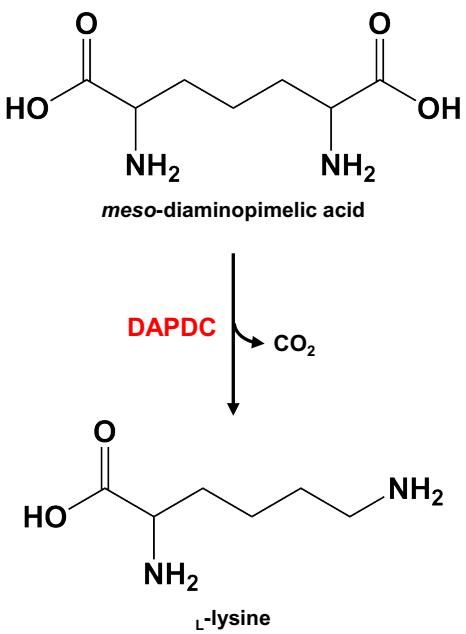

FIGURE 1 | Enzyme reaction of *Cg*DAPDC.

aminotransferase (type IV), and glycogen and starch phosphorylases reactions (type V), respectively. Furthermore, PLP-dependent decarboxylases (PLP-DCs) are divided into four groups according to amino acid sequence and evolutionary origin (Sandmeier et al., 1994). Group I PLP-DC contains glycine DC, and aromatic amino acid DCs are belong to group II PLP-DC. Group III and IV PLP-DCs include DAPDC, lysine DC, ornithine DC, and arginine DC; prokaryotic and eukaryotic enzymes belong to group III and IV PLP-DC, respectively (Sandmeier et al., 1994).

meso-Diaminopimelic acid decarboxylase from *C. glutamicum* (*Cg*DAPDC) is an attractive target for increasing L-lysine productivity through structure based protein engineering. DAPDC utilizes pyridoxal PLP as a cofactor and belong to the group III PLP dependent decarboxylases. Despite the importance of *C. glutamicum* as a producer of L-lysine, structural studies had not been reported on *Cg*DAPDC prior to this study. In this study, we describe the cloning, expression, purification, crystallization and X-ray crystallographic analysis of the *Cg*DAPDC protein.

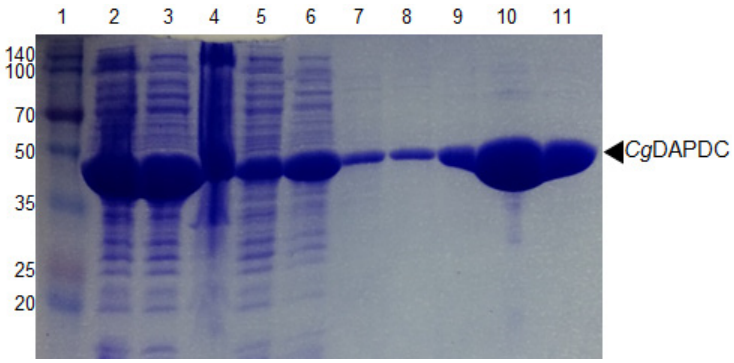

FIGURE 2 | Purification of *Cg*DAPDC. SDS-PAGE of purification of recombinant *Cg*DAPDC protein. Lane 1 shows molecular-weight markers (labelled in kDa). Land 2-11 show the purification procedure of *Cg*DAPDC using Ni-NTA chromatography. Lane 2, whole cell extract; lanes 3 and 4, supernatant and pellet fraction after centrifugation of whole cell extract, respectively; lane 5, flow-through from Ni-NTA column; lane 6 to 9, wash with 0, 10, 20, and 30 mM imidazole, respectively; lane 10 and 11, elution with 300 mM imidazole. Purified *Cg*DAPDC is indicated with an arrow and labeled.

RESULTS AND DISCUSSION

*Cg*DAPDC was purified to apparent homogeneity by Ni-NTA affinity chromatography followed by size-exclusion chromatography. The eluted protein from gel-filtration column, calibrated with Gel Filtration Calibration Kits (GE Healthcare Life Sciences), had a molecular weight of ~ 95 kDa, which corresponds to a dimeric form of *Cg*DAPDC (data not shown). SDS-PAGE of the purified protein showed a single band with a monomeric molecular weight of 47.4 kDa (Figure 2). The *Cg*DAPDC protein was crystallized in 0.8 M sodium citrate tribasic and 0.1 M sodium cacodylate, pH 6.5 (Figure 3). The crystals were transferred to cryo-protectant solution containing 0.8 M sodium citrate tribasic, 0.1 M sodium cacodylate, pH 6.5, and 30% (v/v) glycerol, and the crystals were fished out with a loop larger than the crystals, and flash-frozen by immersion in liquid nitrogen. The crystals of the *Cg*DAPDC diffracted to resolution of 2.4 Å (Figure 4). The *Cg*DAPDC crystals belonged to the space group $P2_12_12$ with unit cell parameters a = 114.54 Å, b = 91.702 Å, c = 95.161, $\alpha = \beta = \gamma = 90°$. Assuming two molecules of CgDAPDC per asymmetric unit, the crystal volume per unit of protein mass was 2.64

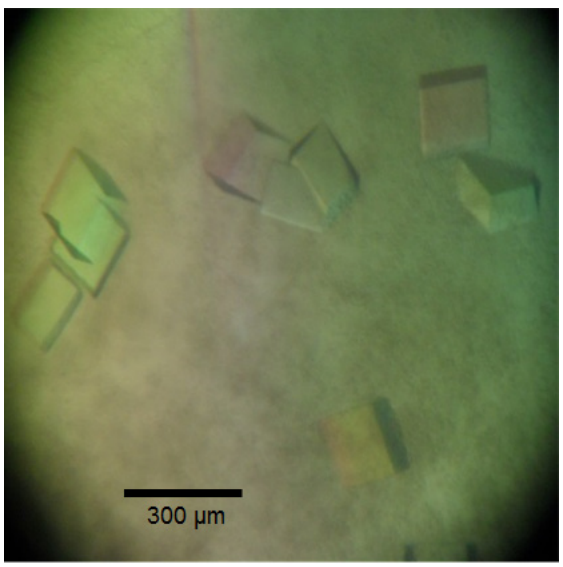

FIGURE 3 | Crystals of *Cg*DAPDC. Crystals of the best quality were produced from the condition 0.8 M sodium citrate tribasic and 0.1 M sodium cacodylate pH 6.5 and grew to maximum dimensions of 0.2 x 0.2 x 0.05 mm within 3 days.

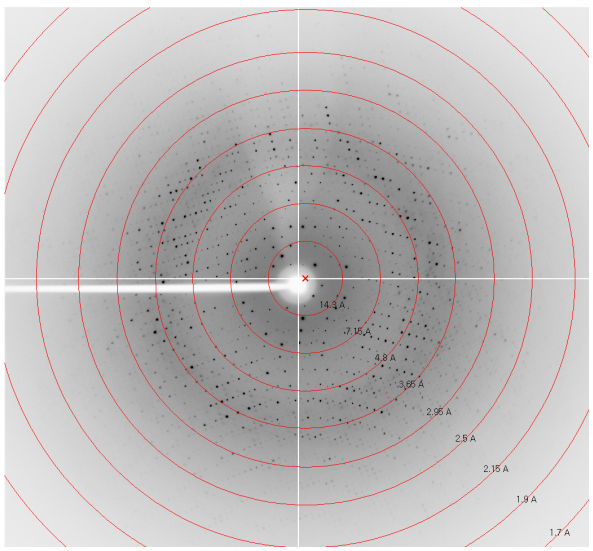

FIGURE 4 | Diffraction pattern of the *Cg*DAPDC crystal. The crystal diffracted to a maximum resolution of 2.4 Å.

TABLE 1 | Macromolecule-production information

Source organism	*Corynebacterium glutamicum* ATCC 13032
DNA source	Chromosomal DNA
Forward primer	GCGCGCATATGGCTACAGTTGAAAATTTCAATGAAC
Reverse primer	GCGCGCTCGAGTGCCTCTAGTGAGAGGATGTCGTC
Cloning vector	pET-30a
Expression vector	pET-30a
Expression host	*E. coli* BL21(DE3)-T1^{R}
Complete amino-acid sequence of the construct produced	MATVENFNELPAHVWPRNAVRQEDGVVTVAGVPLPDLAEEY GTPLFVVDEDDFRSRCRDMATAFGGPGNVHYASKAFLTKTIA RWVDEEGLALDIASINELGIALAAGFPASRITAHGNNKGVEFL RALVQNGVGHVVLDSAQELELLDYVAAGEGKIQDVLIRVKP GIEAHTHEFIATSHEDQKFGFSLASGSAFEAAKAANNAENLNL VGLHCHVGSQVFDAEGFKLAAERVLGLYSQIHSELGVALPEL DLGGGYGIAYTAAEEPLNVAEVASDLLTAVGKMAAELGIDAP TVLVEPGRAIAGPSTVTIYEVGTTKDVHVDDDKTRRYIAVDG GMSDNIRPALYGSEYDARVVSRFAEGDPVSTRIVGSHCESGDI LINDEIYPSDITSGDFLALAATGAYCYAMSSRYNAFTRPAVVSV RAGSSRLMLRRETLDDI LSLEALEHHHHHH

The underlined characters in the primers indicate restriction-enzyme sites.

Å^3 Da^{-1}, which means the solvent content was approximately 53.37% (Matthews, 1968). The structure of *Cg*DAPDC was determined by molecular replacement with the CCP4 version of MOLREP (Vagin and Teplyakov, 2010) using the structure of DAPDC from *Mycobacterium tuberculosis* (*Mt*DAPDC, PDB code 1HKV) as a search model (Gokulan et al., 2003). *Cg*DAPDC has 58% amino acid sequence identity to *Mt*DAPDC. Model building was performed manually using the program WinCoot (Emsley and Cowtan, 2004), and refinement was performed with CCP4 refmac5 (Murshudov et al., 1997). The initial electron density map, which was good quality with backbone atoms well defined by electron density, allowed us to build a three-dimensional *Cg*DAPDC structure. Crystallographic model building and refinement of the structure to 2.4 Å resolution are in progress.

TABLE 2 | Crystallization

Method	Sitting-drop vapor diffusion
Plate type	MRC Crystallization plate (96-well)
Temperature (K)	293
Protein concentration (mg ml^{-1})	60
Buffer composition of protein solution	40 mM Tris-HCl pH 8.0, 150 mM NaCl
Composition of reservoir solution	0.8 M sodium citrate tribasic and 0.1 M sodium cacodylate pH 6.5
Volume and ratio of drop	2 µl; 1:1 ratio of protein and reservoir solutions
Volume of reservoir (µl)	50

METHODS

Production of *Cg*DAPDC

The forward and reverse primers were designed as 5'-GCGCGCATATGGCTACAGTTGAAAATTTCAATGAAC-3' and 5'-GCGCGCTCGAGTGCCTCTAGTGAGAGGATGTCGTC-3' to introduced NdeI and XhoI restriction sites, respectively (underlined). The *Cg*DAPDC coding gene was amplified from *C. glutamicum* strain ATCC 13032 chromosomal DNA by polymerase chain reaction (PCR). The PCR products were then subcloned into pET30a (Novagen) with a six-His tag at the C-terminus. The resulting expression vector pET30a:*Cg*DAPDC was transformed into the *E. coli* BL21(DE3)-T1^{R} strain, which was grown in LB medium containing 50 mg L^{-1} of kanamycin at 310 K. At an OD_{600} of 0.6, *Cg*DAPDC protein expression was induced by the addition of 1 mM isopropyl β-D-1-thiogalactopyranoside (IPTG) and the culture medium was maintained for a further 20 h at 290 K. The culture was then harvested by centrifugation at 4,000 × g for 20 min at 277 K. The cell pellet was resuspended in buffer A (40 mM Tris-HCl, pH 8.0 and 150 mM NaCl) and then disrupted by ultrasonication. The cell debris was removed by centrifugation at 13,500 × *g* for 40 min and the lysate was applied to a Ni-NTA agarose column (QIAGEN). After washing with buffer B (40 mM Tris-HCl, pH 8.0, 150 mM NaCl, and 30 mM imidazole), the bound proteins

TABLE 3 | Data collection and processing

Diffraction source	Beamline 7A, PAL
Wavelength (Å)	0.97933
Temperature (K)	100
Detector	Quantum 270 CCD
Crystal-to-detector distance (mm)	180
Rotation range per image (°)	1
Total rotation range (°)	250
Exposure time per image (s)	1
Space group	$P2_12_12$
a, b, c (Å)	114.65, 92.013, 94.753
α, β, γ (°)	90.0, 90.0, 90.0
Resolution range (Å)	50.00-2.40 (2.44-2.40)[a]
Total No. of reflections	36222
Completeness (%)	96.0 (92.3)[a]
R_{sym} or R_{merge} (%)	10.0 (30.7)[a]
$I / \sigma I$	26.88 (4.07)[a]
Redundancy	4.7 (3.2)[a]

[a]The numbers in parentheses are statistics from the highest resolution shell.

were eluted with buffer C (40 mM Tris-HCl, pH 8.0, 150 mM NaCl, and 300 mM imidazole). Finally, the trace amount of contaminants was removed by size-exclusion chromatography by using a Sephacryl S-300 column (320 mL, GE Healthcare Life Sciences) equilibrated with buffer A. All purification experiments were performed at 277 K and SDS-polyacrylamide gel electrophoresis analysis of the purified proteins shows a single polypeptide of 47.4 kDa corresponding to the estimated molecular weight of the *Cg*DAPDC monomer. The purified protein was concentrated to 60 mg/mL in buffer A. Macromolecule-production information is given in Table 1.

Crystallization of *Cg*DAPDC

Crystallization of the purified *Cg*DAPDC protein was initially performed with commercially available sparse-matrix screens from Hampton Research, Rigaku Reagents, and Molecular Dimensions by using the sitting-drop vapor-diffusion method on the MRC Crystallization plate (Molecular Dimensions) at 293 K. Each experiment consisted of mixing 1.0 μL protein solution (60 mg/ml in 40 mM Tris-HCl, pH 8.0, 150 mM NaCl) with 1.0 μL reservoir solution and then equilibrating this against 50 μL reservoir solution. *Cg*DAPDC crystals were observed from several crystallization screening conditions. After several rounds of crystal improvement, the best quality crystal appeared in 0.8 M sodium citrate tribasic and 0.1 M sodium cacodylate, pH 6.5. Crystallization information is summarized in Table 2.

X-ray diffraction analysis of *Cg*DAPDC

Diffraction data were collected from *Cg*DAPDC crystals on 7A beamline of the Pohang Accelerator Laboratory (PAL, Pohang, Korea), using a Quantum 270 CCD detector (ADSC, USA). The *Cg*DAPDC crystals diffracted to a resolution of 2.4 Å. The data were indexed, integrated, and scaled together using the HKL-2000 software package (Otwinowski and Minor, 1997). The data statistics are summarized in Table 3.

CONFLICT OF INTEREST

The authors have declared that no competing interests exist.

ACKNOWLEDGEMENTS

This work was supported by the New & Renewable Energy Core Technology Program of the Korea Institute of Energy Technology Evaluation and Planning (KETEP) granted financial resource from the Ministry of Trade, Industry & Energy, Republic of Korea (20153030091360). H-F Son was supported by the NRF-2015-Global PhD Fellowship Program of the Korean Government (2015H1A2A1034233).

Original Submission: May 30, 2017
Revised Version Received: Jun 6, 2017
Accepted: Jun 7, 2017

REFERENCES

Becker, J., and Wittmann, C. (2012). Bio-based production of chemicals, materials and fuels -Corynebacterium glutamicum as versatile cell factory. *Curr Opin Biotechnol* **23**, 631-640.

Blombach, B., Riester, T., Wieschalka, S., Ziert, C., Youn, J.W., Wendisch, V.F., and Eikmanns, B.J. (2011). Corynebacterium glutamicum tailored for efficient isobutanol production. *Appl Environ Microbiol* **77**, 3300-3310.

Buschke, N., Schroder, H., and Wittmann, C. (2011). Metabolic engineering of Corynebacterium glutamicum for production of 1,5-diaminopentane from hemicellulose. *Biotechnology Journal* **6**, 306-317.

Chen, Z., Huang, J.H., Wu, Y., and Liu, D.H. (2016). Metabolic engineering of Corynebacterium glutamicum for the de novo production of ethylene glycol from glucose. *Metabolic Engineering* **33**, 12-18.

Emsley, P., and Cowtan, K. (2004). Coot: model-building tools for molecular graphics. *Acta Crystallogr D Biol Crystallogr* **60**, 2126-2132.

Gokulan, K., Rupp, B., Pavelka, M.S., Jr., Jacobs, W.R., Jr., and Sacchettini, J.C. (2003). Crystal structure of Mycobacterium tuberculosis diaminopimelate decarboxylase, an essential enzyme in bacterial lysine biosynthesis. *J Biol Chem* **278**, 18588-18596.

Huang, J., Wu, Y., Wu, W., Zhang, Y., Liu, D., and Chen, Z. (2017). Cofactor recycling for co-production of 1,3-propanediol and glutamate by metabolically engineered Corynebacterium glutamicum. *Sci Rep* **7**, 42246.

Ikeda, M., and Nakagawa, S. (2003). The Corynebacterium glutamicum genome: features and impacts on biotechnological processes. *Appl Microbiol Biotechnol* **62**, 99-109.

Kalinowski, J., Bathe, B., Bartels, D., Bischoff, N., Bott, M., Burkovski, A., Dusch, N., Eggeling, L., Eikmanns, B.J., Gaigalat, L., Goesmann, A., Hartmann, M., Huthmacher, K., Kramer, R., Linke, B., et al. (2003). The complete Corynebacterium glutamicum ATCC 13032 genome sequence and its impact on the production of L-aspartate-derived amino acids and vitamins. *J Biotechnol* **104**, 5-25.

Kumar, R. (2016). Evolutionary Trails of Plant Group II Pyridoxal Phosphate-Dependent Decarboxylase Genes. *Front Plant Sci* **7**, 1268.

Lehmann, K.B.a.N., R.O. (1896). Atlas und Grundriss der Bakteriologie und lehrbuch der speziellen bakteriologischen Diagnostik. (München : J. F. Lehmann).

Matthews, B.W. (1968). Solvent content of protein crystals. *J Mol Biol* **33**, 491-497.

Mimitsuka, T., Sawai, H., Hatsu, M., and Yamada, K. (2007). Metabolic engineering of Corynebacterium glutamicum for cadaverine fermentation. *Biosci Biotechnol Biochem* **71**, 2130-2135.

Murshudov, G.N., Vagin, A.A., and Dodson, E.J. (1997). Refinement of macromolecular structures by the maximum-likelihood method. *Acta Crystallogr D Biol Crystallogr* **53**, 240-255.

Otwinowski, Z., and Minor, W. (1997). Processing of X-ray diffraction data collected in oscillation mode. *Methods Enzymol* **276**, 307-326.

Percudani, R., and Peracchi, A. (2003). A genomic overview of pyridoxal-phosphate-dependent enzymes. *EMBO Rep* **4**, 850-854.

Sagong, H.Y., and Kim, K.J. (2017). Lysine Decarboxylase with an Enhanced Affinity for Pyridoxal 5-Phosphate by Disulfide Bond-Mediated Spatial Reconstitution. *Plos One* **12**. e0170163.

Sagong, H.Y., Son, H.F., Kim, S., Kim, Y.H., Kim, I.K., and Kim, K.J. (2016). Crystal Structure and Pyridoxal 5-Phosphate Binding Property of Lysine Decarboxylase from Selenomonas ruminantium. *Plos One* **11**. e0166667.

Sandmeier, E., Hale, T.I., and Christen, P. (1994). Multiple evolutionary origin of pyridoxal-5'-phosphate-dependent amino acid decarboxylases. *Eur J Biochem* **221**, 997-1002.

Vagin, A., and Teplyakov, A. (2010). Molecular replacement with MOLREP. *Acta Crystallogr D Biol Crystallogr* **66**, 22-25.

Wendisch, V.F., Jorge, J.M.P., Perez-Garcia, F., and Sgobba, E. (2016). Updates on industrial production of amino acids using Corynebacterium glutamicum. *World J Microbiol Biotechnol* **32**. 105.

